Available online at www.sciencedirect.com
ScienceDirect
Polymer 48 (2007) 7000–7007
polymer
www.elsevier.com/locate/polymer

Preparation and characterization of UV-cured epoxy nanocomposites based on *o*-montmorillonite modified with maleinized liquid polybutadienes

G. Malucelli*, R. Bongiovanni, M. Sangermano, S. Ronchetti, A. Priola

Dipartimento di Scienza dei Materiali e Ingegneria Chimica e Unità locale INSTM, Politecnico di Torino, C.so Duca degli Abruzzi 24, 10129 Torino, Italy

Received 19 April 2007; received in revised form 24 August 2007; accepted 7 October 2007
Available online 11 October 2007

Abstract

Polymeric nanocomposites based on an epoxy cycloaliphatic resin and *o*-montmorillonite (Cloisite 30B®) modified by reaction with maleinized liquid polybutadienes were prepared through photopolymerization. The conditions for the *o*-montmorillonite modification were settled. After the reaction, a strong increase of the basal spacing of the nanoclays was evidenced through XRD analysis. The modified clays were dispersed in the epoxy resin (5 wt.%) and subjected to the UV-curing process. The kinetics of the photopolymerization process was evaluated by means of Real-Time FT-IR spectroscopy. The obtained nanocomposites were studied by means of XRD and TEM analyses; the formation of either intercalated or quasi-exfoliated structure was assessed. The thermal and mechanical properties of the cured films were evaluated and correlated to the morphology of the obtained nanocomposites.

Keywords: Cationic photopolymerization; Epoxy nanocomposites; Maleinized polybutadienes

1. Introduction

In the last years, the research activities of a huge number of academic and industrial scientists have been focused on the synthesis and characterization of polymeric nanocomposites. They represent a new class of composite materials, where an inorganic phase is dispersed at a nanoscale level into a polymeric matrix. In the coating field, adding nanostructured fillers is a new procedure to enhance mechanical and thermal resistance, to reduce flammability and to improve the barrier properties of the material, without modifying other important characteristics like transparency and impact resistance [1–5].

The nanofillers are used in small amounts, i.e. below 5 wt.%. Typically they are lamellar silicates, originally aggregated in clusters: the primary particles can be disaggregated by mechanical stirring. If there is affinity between lamellae and polymer chains, intercalation of polymer chains into the crystalline galleries can be achieved. If the intercalation is very effective, it can lead to a total exfoliation of the lamellae, thus obtaining the best effect of the nanofiller on the final properties of the nanocomposite.

The interposition of polymeric chains between the layers of the lamellar silicates can be performed by in situ polymerization during the preparation of the nanocomposite. In this context, the UV-curing technique can be successfully employed; it permits the building up of polymeric thermoset matrices in the presence of the nanofiller, through a fast and environmentally friendly process [6]; thus nanostructured films can be produced [7–9].

Both radical and cationic species can be generated by UV-irradiating a suitable photoinitiator; therefore the reaction mechanism is either radical or cationic.

Previous works have shown the possibility of obtaining intercalated nanocomposites in the presence of epoxy resins, by using cationic photopolymerization [10].

Cationic photopolymerization is receiving renewed interest due to its peculiar characteristics that include the absence of oxygen inhibition, low shrinkage, good adhesion properties and low monomer toxicity [11].

* Corresponding author. Tel.: +39 011 5644621; fax: +39 011 5644699.
E-mail address: giulio.malucelli@polito.it (G. Malucelli).

0032-3861/$ - see front matter © 2007 Elsevier Ltd. All rights reserved.
doi:10.1016/j.polymer.2007.10.008

In Scheme 1 the general mechanism of the photopolymerization of epoxy resins is reported.

The initiation reaction is a multistep process involving first, the photoexcitation of diaryliodonium or triarylsulfonium salts and then the decay of the resulting excited singlet state with both heterolytic and homolytic cleavages. Cations and arylcations generated are very reactive with monomers to form a Brönsted acid, which is the actual initiator of cationic polymerization [12]. Initiation of polymerization takes place by protonation of the epoxy monomer, followed by the addition of further monomer molecules, thus resulting in chain growth reaction. In addition to the usual mechanism, Penczek and Kubisa described a new one (*chain transfer mechanism*) that takes place when the cationic polymerization of epoxides is carried out in the presence of alcohols [13]. This mechanism is also reported in Scheme 1. During the polymerization, the growing ionic chain-end undergoes a nucleophilic attack by the alcohol to give a protonated ether. Deprotonation of this latter species by the epoxy monomers results in the termination of the growing chain and the proton transfer to the monomer can start a new chain.

In order to prepare nanocomposites based on lamellar silicates, often the nanoparticles are partially modified by introducing organic ammonium cations, bearing long alkyl chains, which increase the basal spacing, improve the compatibilization between the filler and the polymer matrix and can enhance the intercalation of the polymers in the nanoclay galleries [14–16].

In this work we prepared novel nanostructured coatings based on an UV-curable epoxy resin. The used nanoclays were modified on purpose, treating a typical *o*-montmorillonite with maleinized liquid polybutadienes (LPBs). Maleinized LPBs are available products, which contain succinic anhydride groups randomly distributed along the polymer chain. They are used for different applications namely as compatibilizers for polymer blends [17,18]. The most suitable experimental conditions (solvent polarity, maleic anhydride content, temperature) for obtaining the modified nanoclays were investigated.

XRD analyses evidenced a strong increase of the basal spacing of the nanoclays after the modification reaction. The modified nanoclays were dispersed at a nanometric level in an epoxy matrix, and then were subjected to UV-curing, obtaining, at particular conditions, quasi-exfoliated structures. The thermal, mechanical and dynamic-mechanical properties of the obtained nanocomposites were investigated.

2. Experimental

2.1. Materials

The epoxy resin (3,4-epoxycyclohexylmethyl-3′,4′-epoxycyclohexan carboxylate, CE) was kindly supplied by Dow Chemicals. Its structure is reported in Fig. 1. As a cationic photoinitiator, a commercially available mixture of antimonate sulfonium salts derived from triphenylsulfonium-exafluoroantimonate (whose structure is reported in Fig. 2), was used. It

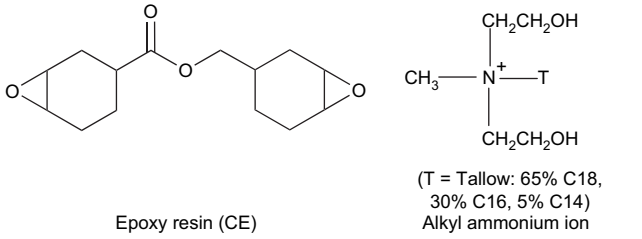

Fig. 1. Structure of the epoxy resin and of the alkyl ammonium ion in Cloisite 30B.

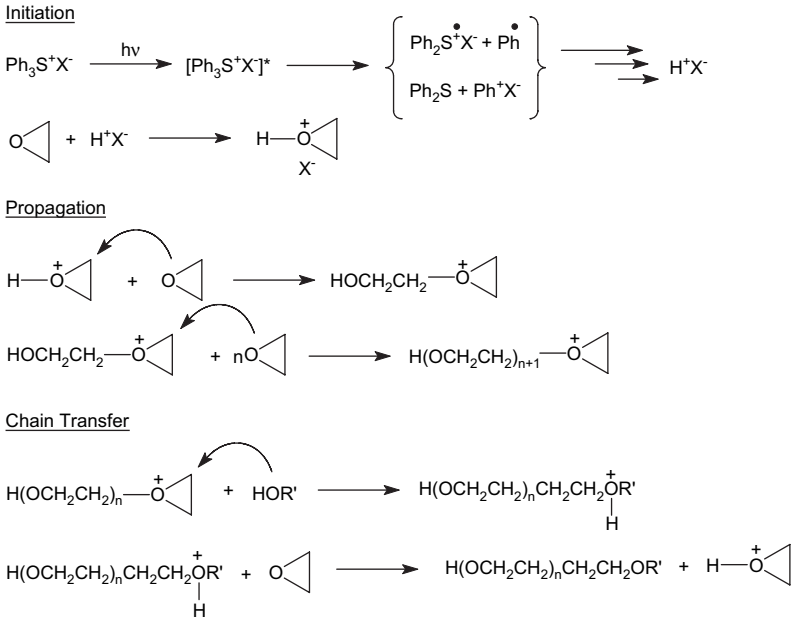

Scheme 1. General scheme of the photopolymerization of epoxy resins.

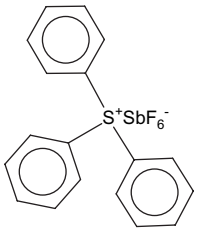

Fig. 2. Structure of triphenylsulfonium-exafluoroantimonate.

was received from Dow (UVI 6976), as a solution in propylene carbonate (50 wt.%); this solution was added to the curable mixtures at a concentration of 4 wt.%.

Some liquid polybutadienes (LPBs), having different microstructures and MW (from 1000 to 5000) and containing 7.5 wt.% of maleic anhydride (MA) were investigated. On the product having MW = 5000 the MA content was varied in the range 2.5–25 wt.%. All the products were kindly supplied by Synthomer Ltd. (UK).

Hereinafter we will indicate maleinized liquid polybutadienes as LPB-*X*-M*Y*, where *X* is a number indicating the kind of starting LPB and *Y* is the wt.% of maleic anhydride (M) present in the product. Some properties of the liquid polybutadienes are reported in Table 1.

A commercially available *o*-montmorillonite (Cloisite 30B®) was purchased from Southern Clay Product Inc. (USA). It contains alkyl ammonium quaternary ions (90 meq of quaternary alkyl ammonium ions per 100 g clay) bearing two hydroxyethyl groups linked to the nitrogen atom. The structure of this alkyl ammonium quaternary salt is reported in Fig. 1.

THF, toluene, *n*-heptane and 2,2-dimethoxy ethane were Aldrich products, used as received.

2.2. Modification of o-montmorillonite with maleinized polybutadienes

The organophilic clay Cloisite 30B was dispersed in different organic solvents (*n*-heptane, toluene, THF, 2,2-dimethoxy ethane) under vigorous stirring for 20 min at room temperature. Then the maleinized polybutadiene was added mantaining a 1:1 stoichiometric ratio between the succinic rings and the $-CH_2CH_2OH$ groups present in the organophilic clay. In the case of 2,2-dimethoxy ethane as solvent, the dispersion was heated at 75 °C for 2 h under vigorous stirring, in the presence of N_2 (gas flow: 10 ml/min). After cooling, the dispersion was filtered and washed with the solvent; then it was dried in oven at 75 °C until a constant weight was reached (yield: 82%).

Table 1
Properties of liquid polybutadienes (LPB)

	MW	Viscosity [Pa s] at		Microstructure [%]			
		25 °C	50 °C	1,2	*Trans* 1,4	*Cis* 1,4	Cyclic
LPB-1	1000	4	0.8	40–55	15–25	10–20	15–20
LPB-2	1300	0.7	0.2	40–50	30–40	15–25	–
LPB-3	5000	4	1.6	10–20	50–60	25–35	–

2.3. Preparation of the UV-cured coatings

Cloisite 30B (as reference) or the products obtained after the reaction with maleinized LPBs were added to the epoxy resin CE at 5 wt.% and dispersed in the resin by using an ultrasonic bath (mod. Branson 1210), at room temperature for 4 h. To the dispersions were added 4 wt.% of UVI 6976 as cationic photoinitiator and exposed to UV-light. For this purpose, the liquid dispersions were coated onto a PET substrate (3 M product, thickness = 36 μm) using a wire-wound applicator, and then the wet films were exposed to UV radiation with a Fusion lamp (H-bulb) in air at a conveyor speed of 5 m/min, with radiation intensity on the surface of the sample of 1400 mW/cm^2. The film thickness was about 150 μm. The UV-cured films were then subjected to a thermal treatment in oven at 80 °C for 2 h; after this treatment their DSC thermograms showed flat traces until 300 °C without any exothermal peak, thus excluding the presence of unreacted epoxy groups.

2.4. Characterization techniques

XRD measurements were performed both on the clays and on the nanocomposites using a Philips X'Pert-MPD diffractometer (Cu Kα radiation; 2θ range: 2–30°; $\Delta 2\theta$ step: 0.02°; step time: 2 s).

Wide angle X-ray scattering (WAXS) analyses were conducted only on the modified clays in order to confirm the basal spacings. Scanning was performed from 1 to 5°, with 0.01° $\Delta\theta$ step and 20 s step time.

The kinetics of the photopolymerization was determined by Real-Time FT-IR spectroscopy, using a Thermo-Nicolet 5700 apparatus. The liquid formulations were coated onto a silicon wafer. The sample was exposed simultaneously to the UV beam, which induces the polymerization, and to the IR beam, which analyzes in situ the extent of the reaction. Because the IR absorbance is proportional to the monomer concentration, conversion vs. irradiation time profiles can be obtained. Epoxy groups' conversion was followed by monitoring the decrease of their absorbance in the region 760–780 cm^{-1}. A medium pressure mercury lamp equipped with an optical waveguide was used to induce the photopolymerization (light intensity on the surface of the sample of about 5 mW/cm^2). All the polymerization reactions were performed at room temperature at constant humidity (25–30% RH).

The gel content of the cured and thermal treated products was determined by measuring the weight loss after 24 h extraction at room temperature with $CHCl_3$.

DSC measurements were performed using a Mettler DSC 30 (Switzerland) apparatus, equipped with a low temperature probe (heating rate: 20 °C/min; temperature precision: ±0.2 °C).

TGA analyses were performed using a Mettler TGA-sDTA 851 Instrument in the range between 20 and 950 °C, with a heating rate of 3 °C/min, in air (temperature reproducibility: ±0.15 °C; mass resolution: 10^{-6} g). The samples were run in duplicate.

Mechanical measurements were carried out through tensile experiments according to ASTM Standard D638, using a Sintech 10/D instrument equipped with an electromechanical extensometer (clip gauge). At least five specimens of each sample were tested; the standard deviation in Young modulus E was 5%.

Dynamic-mechanical experiments (DMTA) were performed on a MKIII Rheometrics Scientific Instrument at 1 Hz frequency in the tensile configuration, from room temperature up to 275 °C, with a heating rate of 5 °C/min. The size of the specimen was 10 × 5 × 0.15 mm. The storage modulus E' and tan δ were measured as a function of temperature. At least three specimens of each sample were tested; the standard deviation in the storage modulus E' was 3%.

The pencil hardness was evaluated on the photocured films according to the standard test method ASTM D 3363.

TEM analyses were performed using a Philips 2010 microscope on microtomized specimens without any specific staining.

3. Results and discussion

3.1. Modification of o-montmorillonite

As reported in the Section 2, Cloisite 30B is a modified montmorillonite containing quaternary ammonium ions having two hydroxyethyl functionalities. They were used as nucleophilic reactive groups toward the succinic rings of the maleinized polybutadienes. A schematic representation of the reaction is reported in Fig. 3.

The reaction was performed in solvents having different polarities. In apolar solvents (*n*-heptane), the reaction was very slow. By increasing the polarity of the solvent, clear evidences of the reaction were obtained; in particular, the best solvent was 2,2-dimethoxyethane. The reaction was monitored by FT-IR analysis perfomed on KBr disks containing the nanoclay powders. In Fig. 4 the typical FT-IR spectra of Cloisite 30B (a) and Cloisite 30B modified with maleinized LPB (b) are compared. The peak located at 1469 cm^{-1} (Fig. 4a) is due to methylene groups of the Cloisite modifier. In the modified nanoclay (Fig. 4b), this peak becomes larger, since it includes also the methylene groups present in LPB. In the (b) spectrum, signals attributable to the presence of ester groups at 1741 cm^{-1} are evident, while the signals related to succinic anhydride rings in the range 1780–1860 cm^{-1} are very feeble. Therefore we can conclude that the reaction of anhydride groups is almost complete.

The modification reaction was confirmed by XRD measurements. In fact the diffraction pattern of Cloisite 30B (Fig. 5) evidences an interlayer distance of 18.4 Å ($d_{(001)}$ peak); when the modification with maleinized LPBs takes place, there is a shift of the diffraction peak toward lower angles, indicating an increase in the interlayer distance.

We have chosen the most convenient maleinized LPB on the basis of its ability to increase the basal spacing of Cloisite 30B; we started with the three different types of LPBs reported in Table 2. They have different microstructures and MW in the range 1000–5000 and contain a typical medium value of MA content (7.5 wt.%).

The XRD results reported in Fig. 5 clearly indicates that LPB-3 gives the highest value of basal spacing. Therefore we focused our investigation on this product, studying the effect of the maleic anhydride content in the range 0–25 wt.%. We found that MA contents lower than 7.5 wt.% give rise to a very low increase of the basal spacing, probably because of the low polarity of such LPBs and subsequently low compatibility with the nanoclay. MA contents higher than 7.5 wt.% evidenced a decrease of the basal spacing of the nanoclay. This behavior can be attributed to the high number of succinic rings per polybutadiene chain, which can decrease the mobility of LPB chains into the galleries of the nanoclay. Therefore we chose LPB-3-M7.5 as the most suitable modifier. It has a MW of 5000 and contains 3.75 succinic rings per PB chain. Thus, in this sample, we have one succinic ring per chain segment having MW = 1330, i.e. per about 25 butadiene repeating units.

3.2. UV-curing process

The kinetics of photopolymerization of the dispersions of the different nanoclays in the epoxy resin was investigated by means of Real-Time FT-IR spectroscopy.

The conversion curves as a function of irradiation time for the neat CE resin and in the presence of 5 wt.% of Cloisite 30B and of Cloisite 30B treated with maleinized LPBs are plotted in Fig. 6. It is evident that the presence of the clays modified with maleinized LPBs practically does not affect the photopolymerization process. Only the systems containing pristine Cloisite 30B show a decrease of both the photopolymerization rate and of the final conversion of the epoxy groups. This behavior can be attributed to the basic character of Cloisite 30B, as previously reported [10]. In fact Cloisite 30B contains free small amounts of quaternary ammonium chloride and of the corresponding tertiary amine. These

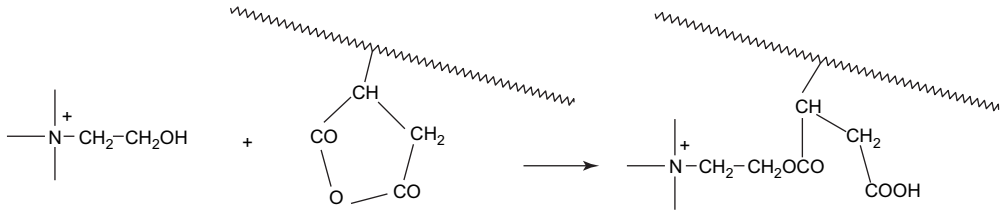

Fig. 3. Schematic representation of the reaction between maleic anhydride and –OH groups.

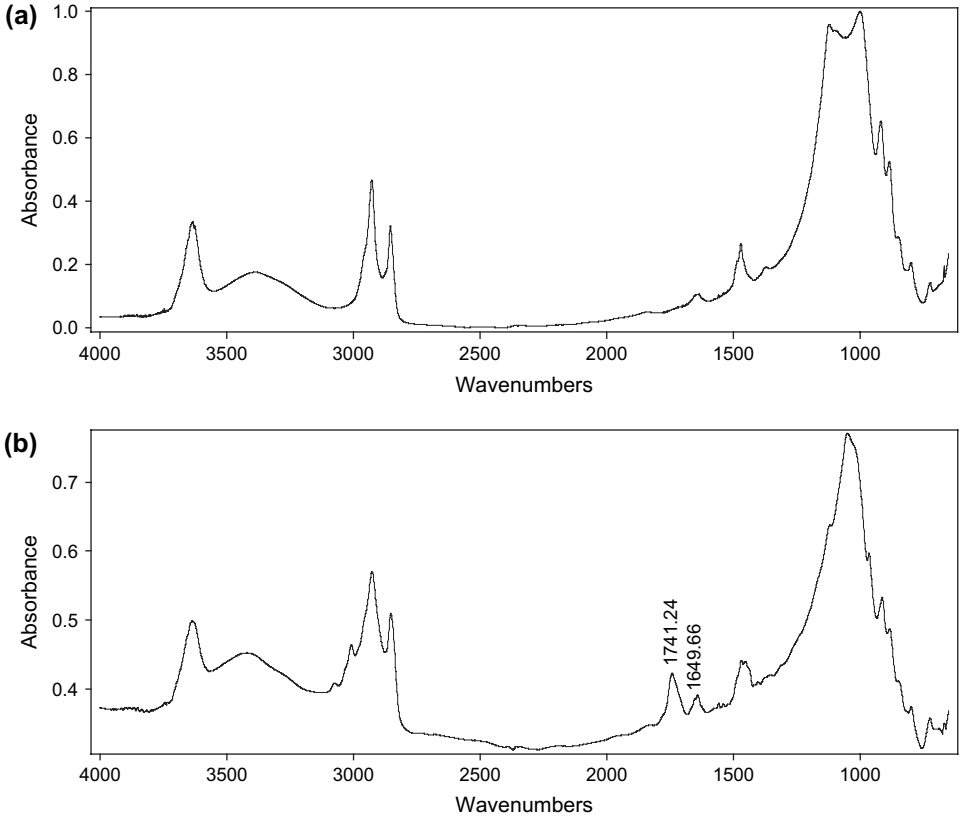

Fig. 4. FT-IR spectra of Cloisite 30B (a) and Cloisite 30B after treatment with LPB-3-M7.5 (b).

impurities are eliminated during the process of modification of Cloisite 30B with maleinized LPBs by washing the final products. Therefore the modified Cloisites do not affect the photopolymerization kinetics.

It can be noted that the modified nanoclays contain acid carboxylic groups, ammonium ions and some residual anhydride groups, which could have an effect on the photopolymerization reaction. In particular, the acid groups are able to react with the propagating cationic species according to a chain transfer reaction, as we reported in Scheme 1. As indicated in the scheme, the propagation reaction is due to a nucleophilic attack of the epoxy monomer on the propagating cation. Since the nucleophilicity of the anhydride groups is very low, they cannot interfere with the polymerization process. Moreover, previous works on cationic photopolymerization of epoxy resins indicated that the rate of polymerization is not affected by the presence of quaternary ammonium ions [10].

Finally in Scheme 1 the formation of free radicals during UV irradiation is indicated. It can be observed that the LPB double bonds have a very poor radical reactivity and cannot be cross-linked by free radicals at room temperature.

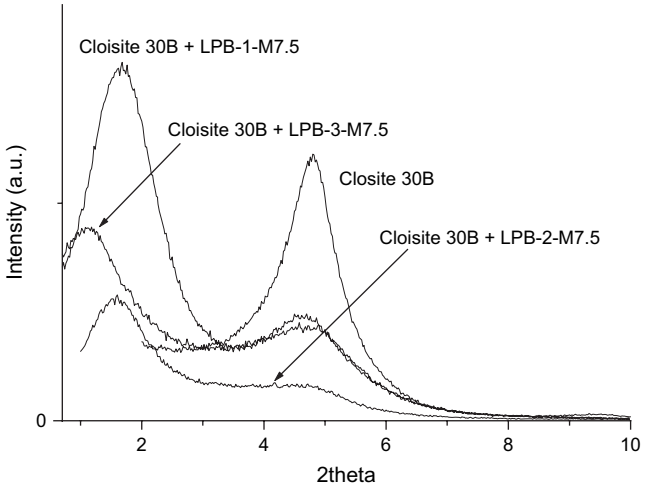

Fig. 5. XRD spectra related to Cloisite 30B treated with different LPBs containing 7.5 wt.% of maleic anhydride.

Table 2
The $d_{(001)}$ spacing values for the different modified nanoclays

Nanoclay	$d_{(001)}$ [Å]	Number of succinic rings per PB chain
Cloisite 30B	18.4	–
Cloisite 30B + LPB-1-M7.5	53.0	0.75
Cloisite 30B + LPB-2-M7.5	55.0	0.98
Cloisite 30B + LPB-3-M7.5	79.8	3.75
Cloisite 30B + LPB-3-M0	18.4	0
Cloisite 30B + LPB-3-M2.5	18.6	1.25
Cloisite 30B + LPB-3-M5	20.0	2.50
Cloisite 30B + LPB-3-M7.5	79.8	3.75
Cloisite 30B + LPB-3-M10	60.2	5.00
Cloisite 30B + LPB-3-M15	34.0	7.50
Cloisite 30B + LPB-3-M25	23.6	12.50

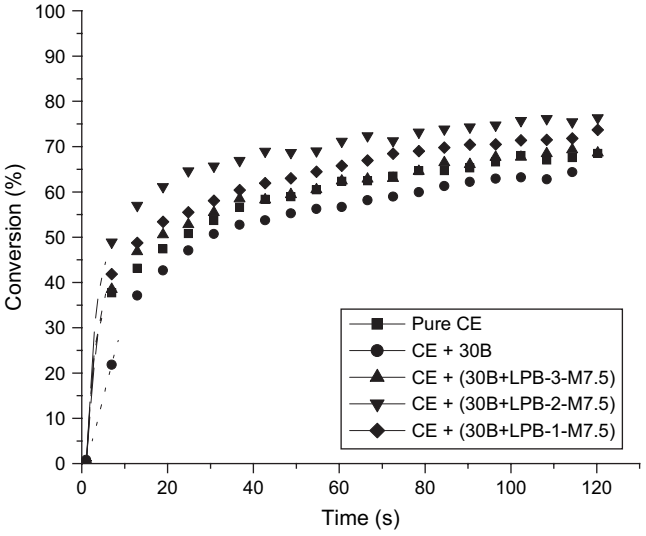

Fig. 6. RT-IR spectra of the UV-curable systems containing different modified clays.

The dispersions of the clays in the epoxy resin were subjected to XRD measurements both before and after the UV-curing process. When Cloisite 30B is dispersed in the liquid resin (Fig. 7), a broad band related to the amorphous structure of the epoxy monomer appears with a maximum at $2\theta = 17.5^{\circ}$ and the clay diffraction peak is found at lower angle with respect to the nanoclay powder. In fact the interlayer distance of the clay increases from 18.4 up to 35 Å. More interesting was, when the epoxy resin was added to the clay modified with LPB-3-M7.5, the liquid dispersion showed no diffraction peak related to the inorganic phase (Fig. 7). The same behavior was found for the other dispersions containing maleinized LPBs (MA content: 7.5 wt.%).

The results indicate that:

- Cloisite 30B-based dispersions show diffraction signals and are likely to have an intercalated structure.
- All the other dispersions based on clays with any LPBs containing 7.5 wt.% of maleic anhydride, show no diffraction signals and could have an exfoliated morphology.

The XRD analyses performed on the same systems after UV-curing (Fig. 8) did not evidence any difference with the features described previously. Therefore the intercalation/exfoliation phenomena are realized in the liquid dispersions and maintained after the UV-curing process.

3.3. Properties of the cured coatings

TEM evaluations were performed on the UV-cured systems. A typical TEM picture related to a cured film containing Cloisite 30B (nanoclay content: 5 wt.%) is reported in Fig. 9. It evidences the presence of different tactoids, formed by intercalated lamellae, well dispersed in the polymer matrix. Fig. 10 reports a magnification of the previous picture, where the intercalation level can be better appreciated. In Fig. 11 a typical TEM picture related to a cured film containing Cloisite 30B + LPB-3-M7.5 (nanoclay content: 5 wt.%) is reported. It evidences a quasi-exfoliated morphology. Moreover, it shows that strong interactions between the lamellae and the polymer matrix occur, giving rise also to some indications of lamellae's deformation.

Also the TEM pictures related to the UV-cured films containing Cloisite 30B modified with maleinized LPB-1 and LPB-2 (with 7.5 wt.% of MA) showed the presence of either intercalated or exfoliated structures.

In Table 3 some thermal and physico-mechanical properties of the UV-cured nanocomposites are collected.

The gel percentage values of all the systems indicate that the coatings are highly insoluble and the curing is complete; Cloisite 30B system shows a slightly lower value (96%).

The T_g values of the cured products were evaluated by DMTA analyses. For all the systems investigated, very high T_gs were found. These values can be explained considering

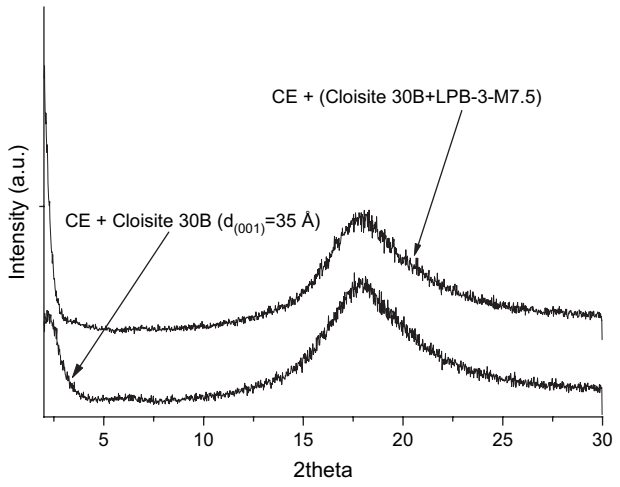

Fig. 7. XRD spectra of CE/Cloisite 30B and CE/(Cloisite 30B + LPB-3-M7.5) before UV curing.

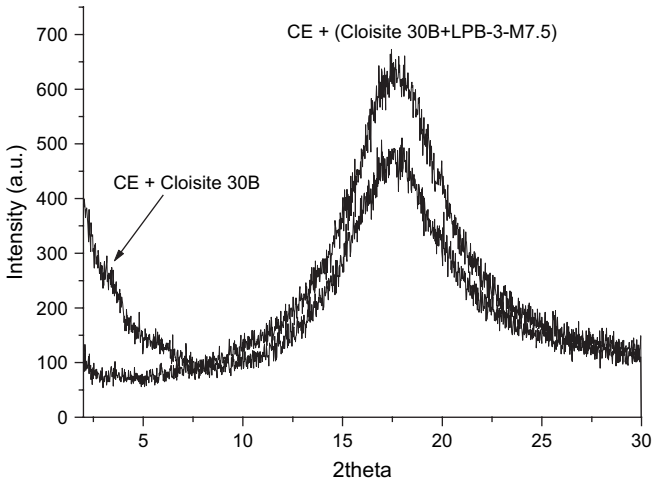

Fig. 8. XRD spectra of CE/Cloisite 30B and CE/(Cloisite 30B + LPB-3-M7.5) after UV curing.

Fig. 9. TEM picture related to an intercalated nanocomposite based on CE and Cloisite 30B.

the high radiation intensity used during the curing process, which can determine local overheating. Moreover, all the samples were subjected to the thermal treatment described in the Section 2. After this treatment the samples showed flat DSC traces without any exothermal peak, indicating that the epoxy groups' conversion was complete. No evidence of T_g steps could be obtained by DSC.

The T_g values were found higher with respect to the neat CE resin for all the systems with the exception of that based

Fig. 10. TEM picture related to an intercalated tactoid of Cloisite 30B in UV-cured CE.

Fig. 11. TEM picture related to a quasi-exfoliated nanocomposite based on CE and Cloisite 30B modified with LPB-3-M7.5.

on pure Cloisite 30B. These results are due to the interactions, which take place between the clay lamellae and the polymer matrix. In fact the mobility of the polymer segments is lowered by the presence of the rigid silicate platelets. When pure Cloisite 30B was used, the T_g of the cured nanocomposite slightly decreased; this result can be attributed either to the lower interactions of the nanoclay with the polymer matrix or to the presence of small amounts of soluble oligomers, revealed by gel%, which act as plasticizers.

Some typical DMTA spectra showing E' and $\tan\delta$ vs. T curves are plotted in Fig. 12.

Similar T_g values were reported very recently in a paper on cationic photopolymerization of CE [19].

The results of the mechanical tests performed on the nanocomposite films (Table 3) evidenced a small increase (about 10%) of E' and Young's moduli. The pure Cloisite 30B system showed lower mechanical properties in agreement with the lower T_g values above reported. The pencil hardness was practically constant and in any case very high.

The thermal stability of the systems was evaluated by means of TGA analyses performed in air. The T_{10} and T_{50} data are collected in Table 4; they indicate that the presence of the modified nanoclays determines an increase of the thermal stability with respect to the neat epoxy resin. In particular the best results were obtained by the system based on LPB-3-M7.5, which had the highest basal spacing. This behavior can

Table 3
Properties of UV-cured nanocomposites (clay content: 5 wt.%)

Sample	Gel (%)	T_g DMTA (°C)	Storage modulus E' (MPa) at 50 °C	Young modulus (MPa) at 25 °C	Pencil hardness
Pure CE	100	203	800	875	6H
CE + 30B	96	186	690	812	6H
CE + (30B + LPB-1-M7.5)	100	213	884	967	7H
CE + (30B + LPB-2-M7.5)	100	210	893	988	7H
CE + (30B + LPB-3-M7.5)	100	227	915	1024	7H

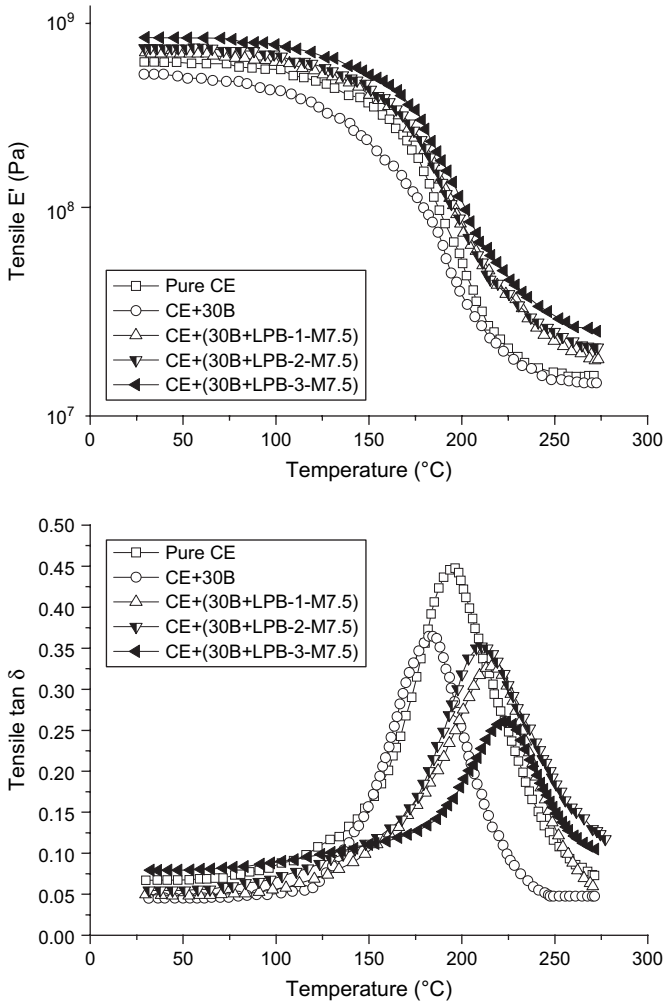

Fig. 12. DMTA spectra of the different nanocomposites.

Table 4
Thermal stability of the different nanocomposites (clay content: 5 wt.%)

Sample	T_{10} [°C]	T_{50} [°C]	Char content (wt.%)
Pure CE	380	430	0
CE + 30B	385	467	3.9
CE + (30B + LPB-1-M7.5)	397	475	4.6
CE + (30B + LPB-2-M7.5)	396	470	4.7
CE + (30B + LPB-3-M7.5)	409	489	4.7

be attributed to the presence of the layered silicates, which decreases the polymer permeability to both oxygen and the volatile decomposition products [1,20].

4. Conclusions

Polymeric nanocomposite systems based on an epoxy cycloaliphatic resin and layered silicates (montmorillonite type), obtained by modifying an *o*-montmorillonite (Cloisite 30B) with maleinized liquid polybutadienes were prepared. The experimental conditions for this reaction were optimized with respect to solvent polarity, maleic anhydride content and temperature. After the treatment, a strong increase of the basal spacing of the nanoclays was evidenced through XRD analysis. The modified clays were dispersed in an epoxy cycloaliphatic resin (5 wt.%) and subjected to UV-curing reaction.

The kinetics of the photopolymerization process, monitored by Real-Time Infrared Spectroscopy, showed very low influence of the presence of the maleinized clays on the curing reaction. The morphology of the UV-cured nanocomposites was investigated by means of XRD and TEM analyses. The formation of either intercalated, or quasi-exfoliated structures was evidenced. The best results were obtained by using, as a modifying agent, a maleinized LPB having MW = 5000 and 7.5 wt.% of MA. This composition corresponds to about one succinic ring per 25 butadiene repeating units in the oligomer chain.

The properties of the final cured films were evaluated through thermal, mechanical and dynamic-mechanical analyses; they were correlated to the intercalated/exfoliated morphology of the nanocomposites revealed by XRD and TEM measurements.

Acknowlegdements

This work was supported by Italian MIUR (FIRB 2001 RBNE017MB5) and Piedmont Regional Funds (Project D26 2004). Dr. P.R. Gardner (Synthomer Ltd, Harlow Essex, UK) is gratefully acknowledged for supplying maleinized LPBs.

References

[1] Giannelis EP. Adv Mater 1996;8(1):29.
[2] Alexandre M, Dubois P, Tao S, Garces JM, Jerome R. Polymer 2002; 43(8):2123.
[3] Ray S, Okamoto M. Prog Polym Sci 2003;28:1539.
[4] Alexandre M, Dubois P. Mat Sci Eng 2000;28:1.
[5] Le Baron PC, Wang Z, Pinnavaia TJ. Appl Clay Sci 1999;15:11.
[6] Fouassier JP, Rabek TF. Radiation curing in polymer science and technology, vol. 1–4. London: Elsevier; 1993.
[7] Decker C, Zahouily K, Keller L, Benfarhi S, Bendaikha T, Baron J. J Mater Sci 2002;37:4831.
[8] Benfarhi S, Decker C, Keller L, Zahouily K. Eur Polym J 2004;40:493.
[9] Decker C, Keller L, Zahouily K, Benfarhi S. Polymer 2006;46:6640.
[10] Bongiovanni R, Mazza D, Ronchetti S, Turcato EA. J Colloid Interface Sci 2006;296(2):515.
[11] Crivello JV. In: Bradley G, editor. Photoinitiators for free radical cationic and anionic photopolymerization. 2nd ed. New York: Wiley; 1998. p. 329.
[12] Fouassier JP, Burr D, Crivello JV. J Macromol Sci 1994;A31:677.
[13] Penczek S, Kubisa P. In: Brunelle J, editor. Ring opening polymerization. Munich: Hanser; 1993. p. 17.
[14] Malucelli G, Ronchetti S, Lak N, Priola A, Dintcheva N, La Mantia FP. Eur Polym J 2007;43:328.
[15] Sasaki A, White JL. J Appl Polym Sci 2003;91:1951.
[16] Liang G, Xu J, Bao S, Xu W. Polymer 2004;91:3974.
[17] Krulis Z, Kokta BV, Horak Z, Michalkova D, Fortelny I. Macromol Mater Eng 2001;286:156.
[18] Mounir A, Darwish NA, Shehata A. Polym Adv Technol 2004;15:209.
[19] Fernandez-Francos X, Salla JM, Cadenato A, Morancho JM, Mantecon A, Serra A, et al. J Polym Sci Part A Polym Chem 2007;45:16.
[20] Lepoittevin B, Pantoustier N, Devalckenaere M, Alexandre M, Calberg C, Jerome R, et al. Polymer 2003;44:2033.